# A fiber optic ultrasonic sensing system for 2D temperature field monitoring using optically generated acoustic waves

Jingcheng Zhou[a], Xu Guo[b], Tong Ma[c], Cong Du[a], Yuqian Liu[c], Chengyu Cao[c] and Xingwei Wang[a, b,*]

[a] Dept. of Biomedical Engineering and Biotechnology, University of Massachusetts Lowell, One University Avenue, Lowell, MA, USA 01850; [b] Dept. of Electrical and Computer Engineering, University of Massachusetts Lowell, One University Avenue, Lowell, MA, USA, 01850; [c] Dept. of Mechanical Engineering, University of Connecticut, 2131 Hillside Road, Storrs, CT, USA 06269

## ABSTRACT

In this paper, we present a novel fiber optic ultrasonic sensing system to conduct a 2D temperature field monitoring. The fiber optic ultrasonic sensing system was used as an ultrasonic pyrometer to measure the temperature field. The ultrasonic pyrometer was based on the thermal dependence of the speed of sound in air. The speed of a sound wave traveling in a medium was proportional to the medium's temperature. A fiber optic ultrasonic generator and a microphone were used as the ultrasonic signal generator and receiver, respectively. A carbon black-Polydimethylsiloxane (PDMS) material was utilized as the photoacoustic material for the fiber optic ultrasonic generator. A test was performed outside of a lab furnace, the testing area temperature range was from 26°C to 70°C. A 2D temperature field was mapped. The 2D temperature field map matched with the reference thermocouple results. This system could lead to the development of a new generation temperature sensor for temperature field monitoring in coal-fired boilers or exhaust gas temperature monitoring for turbine engines.

**Keywords:** fiber optic sensor, 2D temperature field monitoring, ultrasonic pyrometer, temperature distribution, photoacoustic

## 1. INTRODUCTION

In various industries, temperature monitoring is critical, such as food inspection, pharmaceuticals, oil/gas exploration, environmental and high-voltage power systems. In some applications, temperature sensors are required which are immune to electromagnetic interference, durability to harsh environments, remote sensing capability, multiplexing capability, wide operating range, and allow long-distance interrogation without the electrical interface. Fiber optic sensors provide a good solution for many of these challenges [1-4]. However, most of the fiber optic sensors are used for point measurement, whether it is single or multipoint measurement.

In some applications, such as temperature field monitoring in coal-fired boilers or exhaust gas temperature monitoring for turbine engines, the industry wants a 2D temperature distribution profiler rather than some temperature points. Traditionally, the industry is using electronic transducers as the acoustic pyrometers for the temperature field monitoring. However, these electronic transducers have some drawbacks. They cannot survive in the boiler high temperature environment, and also have electromagnetic interference.

In this paper, for the signal generator part, the electronic transducer has been replaced by fiber optic sensor [5-13]. Since it is fabricated by optical fibers, the fiber optic signal generator can survive in a higher temperature than the traditional electronic transducers. A carbon black-Polydimethylsiloxane (black PDMS) material was utilized as the photoacoustic material for the fiber optic ultrasonic generator. A test was performed outside of a lab furnace, the testing area temperature range was from 26°C to 70°C. A 2D temperature field was mapped. The 2D temperature field map matched with the reference thermocouple results.

*Xingwei_Wang@uml.edu; phone 1 978 934-1981; fax 1 978 934-3027; faculty.uml.edu/xwang/

Photonics and Education in Measurement Science 2019, edited by Maik Rosenberger,
Paul-Gerald Dittrich, Bernhard Zagar, Proc. of SPIE Vol. 11144, 111440W
 · doi: 10.1117/12.2531133

This paper is organized as follows: Section 2 presents the methodology. Section 3 describes the experimental setup and results. Section 4 concludes the paper.

## 2. METHODOLOGY

The fiber optic ultrasonic generator is based on the photoacoustic (PA) principle. This principle relates to a material that excited by optical irradiation. The energy of light radiation is absorbed in the material and is converted to local temperature rise. This temperature rise will result in ultrasonic waves through the thermoelastic effect. Ultrasonic waves can be generated by periodically exciting the material with optical energy.

In this paper, black PDMS (20% carbon black + 80% PDMS) material was used as the photoacoustic material and coated on a glass slide [14-17]. Light launched from a 532 nm Nd:YAG nanosecond laser (Surelite I-10, Continuum) traveling through a 1000/1035 µm optical fiber was shone onto the black PDMS and the ultrasonic signal was thus generated. Figure 1 shows an ultrasonic signal that was generated by the fiber optic ultrasonic generator.

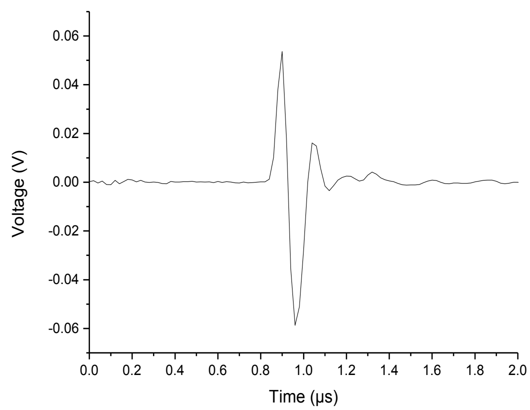


Figure 1. The ultrasonic signal generated by the fiber optic generator.

## 3. EXPERIMENTS AND RESULTS

This test was to use the fiber optic ultrasonic sensing system to measure the temperature in air and reconstructed the 2D temperature field. The experimental setup is shown in figure 2. A fiber optic ultrasonic generator was used as the signal generator. Black PDMS material was coated on a glass slide. Light launched from a 532 nm Nd:YAG nanosecond laser (Surelite I-10, Continuum) travelled through a 1000/1035 µm optical fiber was shone onto the black PDMS and this generated the ultrasonic signal. A microphone (TMS 130C21, PCB) was used as the signal receivers. The generator and receiver were fixed on the two moving stages. The generator and the receiver were set on the same height. The test was performed outside of a lab furnace. A reference thermocouple (KHXL-116G-RSC-24, OMEGA) was used in this test.

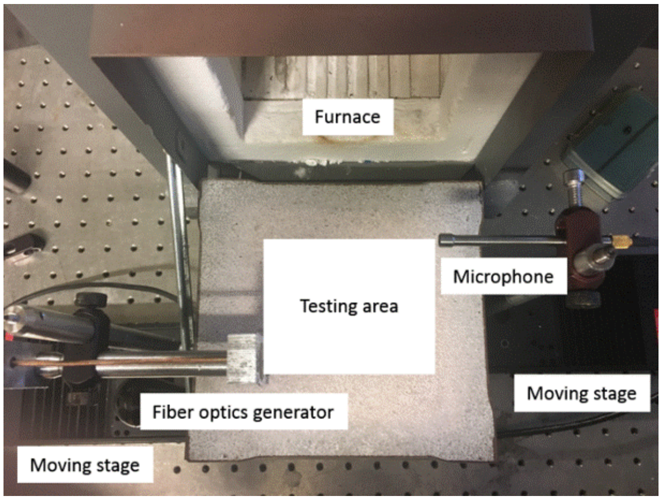


Figure 2. Experimental setup.

The testing area is shown in figure 3. It is a rectangle area (8cm * 6cm). The receiver (Microphone) was set on 5 different locations through the moving stage. The generator was set in 3 different locations. The blue points were the testing generator and receiver locations. We set the generator at the location 0, 0.5 and 1, and the receiver at the location 8, 7.5, 7, 6.5 and 6. Fifteen different paths were tested in the test. Data were collected at room temperature (26°C) and high temperature (furnace set temperature at 250°C) respectively. The reference thermocouple temperature map is shown in figure 4.

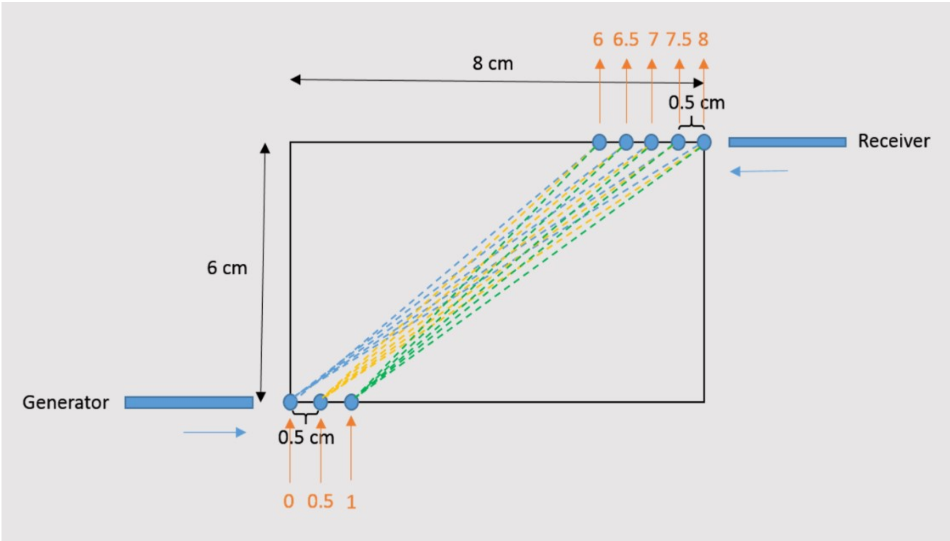


Figure 3. Testing area.

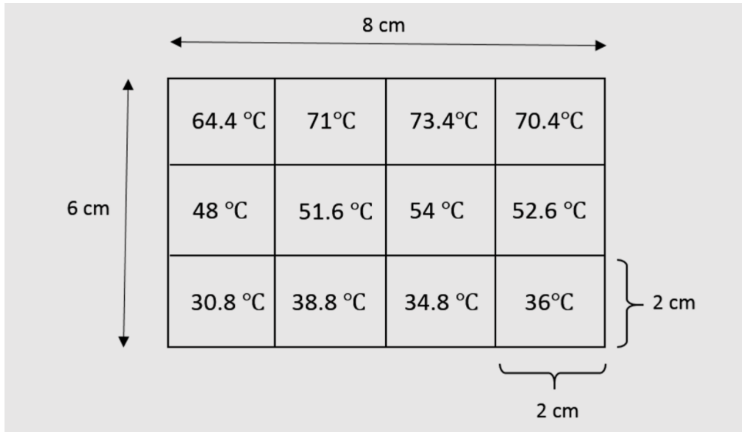


Figure 4. Reference temperature map recorded by the thermocouple.

As shown in figure 5, it is the location (0, 8) (generator at location 0 and receiver at location 8) ultrasonic signal data. The top one is the signal at room temperature (26°C), the bottom one is the signal at high temperature (furnace set temperature at 250°C). According to the website tool [18], the speed of sound $v_1$ at 26°C was calculated as 346.71 m/s. The travel time $t_1$ was 283 µs at room temperature from figure 5. The generator and receiver travel real distance s was calculated as 9.81 cm based on equation (1).

$$s = t_1 v_1 \tag{1}$$

The travel time $t_2$ was 276 µs at high temperature from figure 5, so the speed of sound was calculated as 355.43 m/s based on equation (2).

$$v_2 = s/t_2 \tag{2}$$

Based on the website tool, the temperature is 41.24 °C when the speed of sound at 355.43 m/s. The average temperature for this path was 41.24 °C. 15 paths temperature data were calculated by using the ultrasonic signal traveling time as shown in table 1. The measurement error was ± 1°C. A 2D temperature field was mapped based on the 15 temperature paths as figure 6. The 2D temperature field map matched with the reference thermocouple results [19-21].

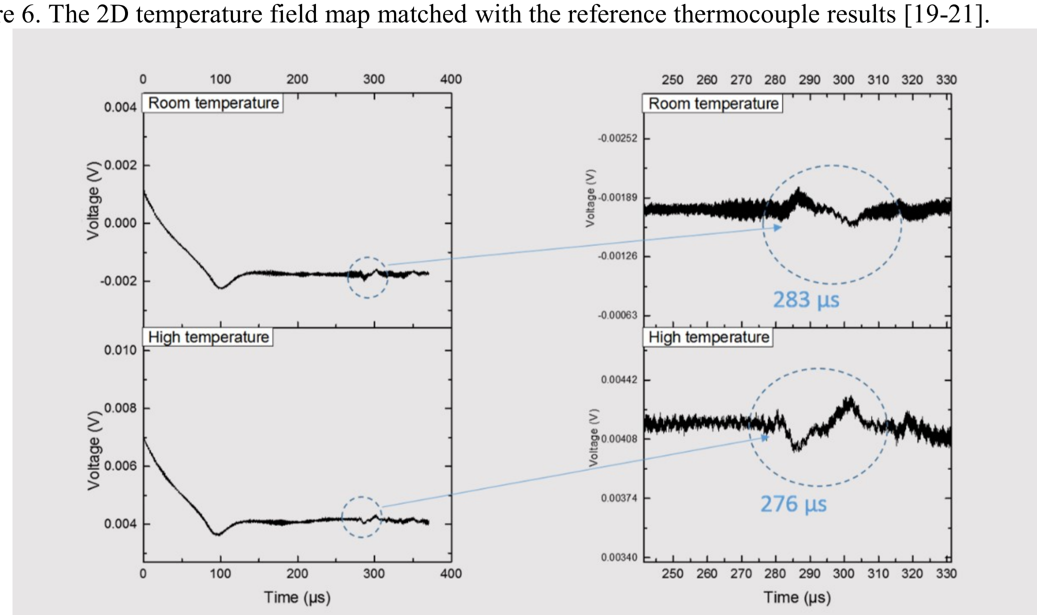


Figure 5. Location (0, 8) ultrasound signal.

Table 1. 15 paths temperature information.

| Location | Room Temperature Traveling Time (μs) | Testing Temperature Traveling Time (μs) | Average Temperature (°C) |
|---|---|---|---|
| (0, 8) | 283 | 276 | 41.24 |
| (0, 7.5) | 271 | 267 | 35.02 |
| (0, 7) | 259 | 250 | 47.93 |
| (0, 6.5) | 247 | 244 | 33.40 |
| (0, 6) | 236 | 233 | 33.75 |
| (0.5, 8) | 270 | 264 | 39.75 |
| (0.5, 7.5) | 260 | 256 | 35.42 |
| (0.5, 7) | 248 | 242 | 41.02 |
| (0.5, 6.5) | 236 | 232 | 36.41 |
| (0.5, 6) | 224 | 219 | 39.82 |
| (1, 8) | 259 | 255 | 35.46 |
| (1, 7.5) | 248 | 244 | 35.89 |
| (1, 7) | 236 | 232 | 36.41 |
| (1, 6.5) | 225 | 221 | 36.93 |
| (1,6) | 215 | 211 | 37.45 |

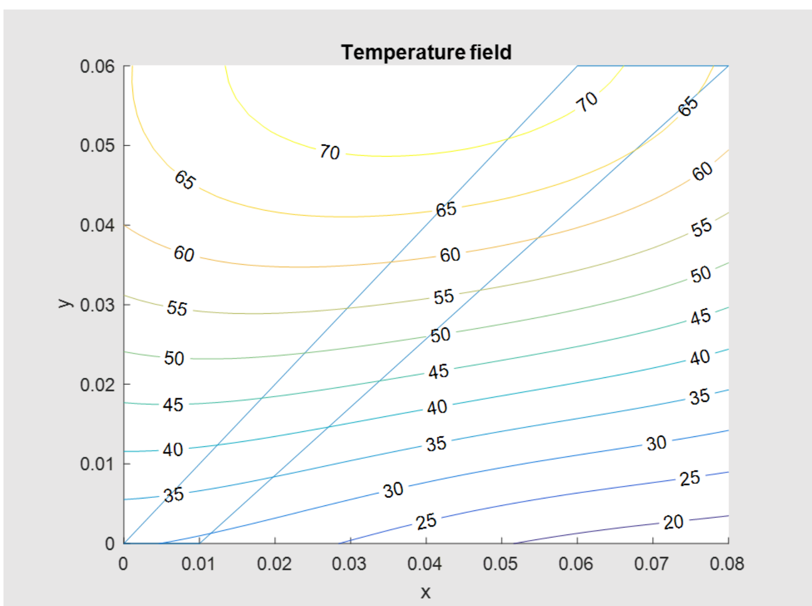


Figure 6. A 2D temperature field reconstruction results.

# 4. CONCLUSION

In this paper, we have designed, fabricated, and characterized the fiber optic ultrasonic sensing system to measure the temperature in air and reconstructed the 2D temperature field. This system is the active non-contact optical fiber sensing system using optically generated acoustic signals to operate in the air temperature environment. The 2D temperature field map matched with the reference thermocouple results. In summary, this fiber optic ultrasonic sensing system could lead to the development of a new generation temperature sensor for temperature field monitoring in coal-fired boilers or exhaust gas temperature monitoring for turbine engines.

## REFERENCES


[1] Lowder, Tyson L., Kevin H. Smith, Benjamin L. Ipson, Aaron R. Hawkins, Richard H. Selfridge, and Stephen M. Schultz., “High-temperature sensing using surface relief fiber Bragg gratings,” IEEE photonics technology letters 17(9), 1926-1928 (2005).

[2] Feng, Y., Zhang, H., Li, Y. L., and Rao, C. F., “Temperature sensing of metal-coated fiber Bragg grating. IEEE/ASME Transactions on mechatronics,” 15(4), 511-519 (2010).

[3] Shen, Y., Wang, Y., Tong, L., and Ye, L., “Novel sapphire fiber thermometer using fluorescent decay,” Sensors and Actuators A: Physical, 71(1-2), 70-73 (1998).

[4] Shen, Y., Tong, L., Wang, Y., and Ye, L., “Sapphire-fiber thermometer ranging from 20 to 1800° C,” Applied optics, 38(7), 1139-1143 (1999).

[5] Zou, X., Wu, N., Tian, Y., and Wang, X., “Broadband miniature fiber optic ultrasound generator,” Optics express, 22(15), 18119-18127 (2014).

[6] Wu, N., Zou, X., Zhou, J., and Wang, X., “Fiber optic ultrasound transmitters and their applications,” Measurement, 79, 164-171 (2016).

[7] Zhou, J., Wu, N., Ma, T., Guo, X., Du, C., Liu, Y., Cao, C., and Wang, X., “Proof of concept temperature field monitoring using optically generated acoustic waves sensing,” Proceedings of the 59th ISA POWID Symposium, 27-30 (2016)

[8] Zhou, J., Guo, X., Du, C., Cao, C., and Wang, X., “A Fiber Optic Ultrasonic Sensing System for High Temperature Monitoring Using Optically Generated Ultrasonic Waves,” Sensors, 19(2), 404 (2019).

[9] Zhou, J., Guo, X., Du, C., Wu, N., and Wang, X., “Characterization of ultrasonic generation from a fiber-optic sidewall,” Proc. SPIE 10654, 106540U (2018).

[10] Zhou, J., Guo, X., Du, C., Wu, N., and Wang, X., “High temperature monitoring using a novel fiber optic ultrasonic sensing system,” Proc. SPIE 10639, 1063910 (2018).

[11] Bi, S., Wu, N., Zhou, J., Ma, T., Liu, Y., Cao, C., and Wang, X., “Ultrasonic temperature measurements with fiber optic system,” Proc. SPIE 9803, 98031Y (2016).

[12] Zhou, J., Guo, X., Du, C., Li, S., Marthi, P., Ma, T., Liu, Y., Edberg, C, Lou, X., Cao, C., and Wang, X. “Ultrasonic wave-based all optical fiber sensor system for high temperature monitoring in a boiler.” Proceedings of the 61th ISA POWID Symposium, 1(5) (2018).

[13] Tang, Q., Twumasi, J. O., Hu, J., Wang, X., and Yu, T., “Finite element simulation of photoacoustic fiber optic sensors for surface corrosion detection on a steel rod,” Proc. SPIE. 10599, 105991N (2018).

[14] Bi, S., Wu, N., Zhou, J., Zhang, H., Zhang, C., and Wang, X., “All-optically driven system in ultrasonic wave-based structural health monitoring,” Proc. SPIE. 9803, 98030K (2016).

[15] Zhou, J., Wu, N., Wang, X., Liu, Y., Ma, T., Coxe, D., and Cao, C. “Water temperature measurement using a novel fiber optic ultrasound transducer system,” In 2015 IEEE International Conference on Information and Automation, 2316-2319 (2015).

[16] Guo, X., Wang, X., Wu, N., Zhou J., and Du, C., “Ultrasound generation from side wall of optical fibers,” In ICOCN 2017 (2017).
[17] Zhou, J., Wu, N., Wang, X., “Ultrasound generation from an optical fiber sidewall,” Proc. SPIE. 9803, 98031U (2016)
[18] Sengpielaudio <:http://www.sengpielaudio.com/calculator-speedsound.htm > (28 April 2019).
[19] Hu, J., AlZeyadi, A., Tang, Q., and Yu, T., “Characterization of dielectric constant of masonry wall using synthetic aperture radar imaging.” Proc. SPIE 10971, 109710S (2019).
[20] Chen, Y., Zhang, B., Zhang, N., and Zheng, M., “A condensation method for the dynamic analysis of vertical vehicle–track interaction considering vehicle flexibility,” Journal of Vibration and Acoustics, 137(4), 041010. (2015).
[21] Chen, Y., Joffre, D., and Avitabile, P., “Underwater dynamic response at limited points expanded to full-field strain response. Journal of Vibration and Acoustics”, 140(5), 051016 (2018).